



A TWO-DIMENSIONAL DRIFT CHAMBER

M. Atac, R. Bosshard*

Fermi National Accelerator Laboratory

S. Erhan†, P. Schlein

University of California, Los Angeles

June 30, 1976

ABSTRACT

A two-dimensional drift chamber with a thin printed-circuit tape delay line positioned between two close sense wires was built and tested in a muon beam at Fermilab. A spacial resolution of $\sigma = 1 \text{ mm}$ in the coarse dimension is obtained with a collimated Fe^{55} source and $\sigma = 3 \text{ mm}$ in the muon beam.

* Presently at Laboratoire Accelérateur Linear, Orsay, France

† Fellow of Turkish Ministry of Education



Introduction

Obtaining two-dimensional associated coordinates of a charged particle track from a proportional or a drift chamber cell is desirable, especially for high multiplicity experiments. Multi-track coordinate ambiguities and the need for rotated (u,v) chambers are removed and computing costs are decreased.

Breskin, et al,¹ have proposed a chamber configuration which offers two-dimensional readout capability by positioning a helical delay line between two closely-spaced sense wires. The two sense wires solve the left-right ambiguity as suggested by Walenta, et al.² In the present paper, we describe results obtained from a similar chamber but instead use a thin printed circuit tape delay line between the two closely-spaced sense wires. The delay line has good transmission characteristics, with an impedance of 75Ω and minimal dispersion and appears to have improved longitudinal coordinate resolution and certain geometrical and constructional advantages.³⁻⁶ References 3 to 6 contain other work on delay readout techniques.

The delay line serves as an electric field-shaping electrode and picks up an induced pulse when a pulse occurs on one of the neighboring sense wires. This pulse then travels on the delay line in two opposite directions toward the ends. A measurement of time difference between pulses obtained from the ends is a measure of the longitudinal coordinate along the delay line. This coordinate can be measured with resolutions of $\sigma = 1\text{mm}$ with a source and 3.0 mm in a muon beam.

-2-

The transverse coordinate is measured from the drift time of the primary electrons. Earlier results show that this coordinate can be measured with resolutions of 60-100 microns. ⁷⁻⁹

Chamber Construction

Figure 1 shows the cross-sectional view of the two-dimensional drift chamber. The chamber has a total sensitive area of 5 cm x 30 cm. The total length of the tape delay line is 50 cm, thus, 20 cm of the line extended outside the sensitive area. The fact that no detectable dispersion was observed is thus characteristic of the 50 cm rather than 30 cm.

The potentials applied to the chamber are indicated in the figure. The potentials can be adjusted to balance the electrostatic forces on the sense wires and the delay line. Thus it would be possible to construct large chambers of this type without supporting the signal wires.

The construction of the chamber is relatively easy. The delay line is glued in a slit of a G-10 support under a constant tension of 100 grams using Eastman 910 glue. The signal wires are soldered in position on a printed circuit strip under a constant tension of 60 grams, with a positioning accuracy of 10 microns. The field shaping wire planes are on two separate G-10 frames. The entire chamber was placed in an aluminum box with 25 micron aluminum foil windows.

-3-

An earlier report ⁽¹⁰⁾ was written on a similar type of chamber with the delay line taking the place of the drift wire. The spatial resolution obtained from this chamber was poor, $\sigma(\text{rms}) = 5 \text{ mm}$, compared with that obtained from the chamber reported here. This difference is due to the larger distance between the delay line and the sense wires.

The Delay Line

The delay line has two characteristic features. It provides a uniform electric field and it senses the induced signal. Desirable characteristics of such a delay line are:

- a) High characteristic impedance Z to achieve primarily good signal to noise ratio, which is proportional to $Z^{\frac{1}{2}}$.
- b) Good coupling efficiency η (described below).
- c) Long delay time, τ , per unit length.
- d) A reasonable balance among signal losses due to d.c. resistance, skin effect, dispersion and the mass of the conductive material to minimize interactions.

Most of the above objectives are achieved in a flat geometry by using a printed circuit technique. This is illustrated in Figure 2a. The delay lines are photo-etched on both sides of Copper-cladded (25μ thick) Mylar (65μ thick) strips. The rest of the dimensions are given with the figure. The conductive planes on a strip are shifted by a half period in order to boost the inductance L while maintaining a constant capacitance C , thus simultaneously increasing impedance Z and the delay time τ .

-4-

Figure 2b shows how this takes place. The current I in the two conductors (in the region where they overlap) are in the same direction thereby enhancing the mutual inductance. The inductance of an iterative loop can be seen to be four times the inductance of a single loop. For the lines considered here, the single loop inductance is three times the inductance of the strip (non-shifted zig-zag) of the same length. As a result, we get a factor of 12 in inductance, thus an increase of about a factor of 3.5 in Z and τ . Some details on the delay lines are given in Reference 11.

The coupling efficiency η of the delay line looking toward the anode wire is related by the difference between the induced charge on the forward zig-zag plane q_f and that seen by the backward zig-zag plane q_b . Since these charges are proportional to the capacitances c_f and c_b , we define η to be:

$$\eta = \frac{C_f - C_b}{C_f + C_b} \quad (1)$$

The η is also dependent on the ratio of the width W over the spacing S of the delay line. To improve η the ratio W/S of the forward plane can be increased relative to that of the backward plane. In this way, coupling efficiency of 80% has been achieved without losing much of the properties of the line.

The skin effect and the d.c. resistance are mainly the limiting factors in choosing a practical length for a delay line.

-5-

To see the characteristic skin effect, we take the time for a step function to rise to 50% of its amplitude (from the theory of long cables):¹²

$$t_{50} = \frac{\rho\mu}{4Z^2} \left(\frac{l_o}{W} \right)^2 \quad (2)$$

Where ρ is the resistivity, μ is the permeability, Z is the characteristic impedance, W is the width, and the l_o is the total length of the conductor in one plane. Four times this value is taken in the case of the delay line. For copper, we obtain the following practical formula in MKS units:

$$t_{50} \approx \frac{2 \cdot 10^{-4}}{Z^2} \left(\frac{l_o}{W} \right)^2 \quad (3)$$

We see from this expression that it is important to achieve a high impedance Z for our 50 cm long delay. We get $t_{50} \approx 3.6$ nsec from the conductor of 250 μ width and $l_o \approx 8$ m with an impedance of 75 Ω .

Test With A Source

A well-collimated 5.9keV x-ray of Fe⁵⁵ was used to obtain the following results with 50% Argon + 50% Ethane (C₂H₆) gas mixture flowing through the chamber. The electron drift velocity is saturated in this gas at fields above 0.8kV/cm at atmospheric pressure. The chamber is operated in the proportional region during the entire test. The 5.9keV x-ray line and the Argon escape line are clearly seen in Figure 3. An integrating

-6-

charge amplifier and a pulse height analyzer were used to obtain the picture.

A balance to unbalance transformer was coupled to each end of the delay line. The pulses obtained through the transformer were amplified using the circuit shown in Figure 4. The pulses from one of the sense wires and one end of the delay line are shown in Figures 5a and b respectively. The induced pulse height is seen to be about 20% of the anode pulses. Pulse attenuation factor of the 50 cm line is about 20% for the induced pulses.

The collimated source was moved in steps of 1 cm along the drift chamber cell. Figure 6 shows some delay time spectra obtained from the difference time measurements which are measured by a time-to-amplitude converter and stored in a pulse height analyzer. Figure 7 shows a good linear relation between the position of the source and the mean delay time difference. A sensitivity of 4 nsec delay time per cm is obtained. A position resolution of $\sigma = 1$ mm. is found using the source.

Tests In A Muon Beam

Further tests were carried out at the M6 West branch beam line of the Meson Laboratory using muons. The beam was defined by three pairs of multi-wire proportional chamber (MWPC) x and y planes of Experiment 260. Figure 8 shows the overall view of the set up. Delay times were measured using a LeCroy TDC,

-7-

(time digitizer) on line to a PDP-11 computer for different chamber positions relative to the beam. The trigger pulse obtained from three plastic scintillators in coincidence provided the start signal for the TDC. The data from the MWPC and TDC were analyzed off-line. Figure 9 shows the position accuracy with respect to the track position as determined from a nearby 1 mm wire spacing MWPC. A position accuracy of σ (rms) = 3.0 mm is obtained over the entire range.

The delay line system efficiency for obtaining a signal above the noise level was measured to be better than 98% for the muon beam. This number includes detection inefficiencies from the sense wires. The drift chamber is found to be fully efficient across the entire drift range including the space between the delay line and sense wires as expected.

Conclusions

1. The chamber removes left-right track ambiguities with the two sense wires for a large fraction of the events. Ninety-five percent removal of this ambiguity can be achieved by reducing the distance between the delay line and the sense wires to 1 mm. This would further increase the induced signal height and the spatial accuracy.

2. The electron drift time across the cell and the track position along the delay line can be obtained from the delay line alone. The position along the delay line is obtained from the difference time measured at both ends. The sum of the delay times gives the drift time. The resolution is, of course, worse

-8-

than furnished by the sense wire, but the redundancy may be useful in some cases.

3. Track points are available for use by fast on-line processor circuits.

4. The delay line is being made commercially.

Acknowledgements

The authors would like to express their appreciation to M. Hrycyk and J. Urish for assistance in constructing the chamber, to Q. Kerns for useful discussions, and to the Experiment 110/260 group, especially J. Rohlf and R. Stanek for their assistance during the tests.

REFERENCES

1. A. Breskin, G. Charpak, F. Sauli and J.C. Santiard, Nucl. Instr. and Meth. 119 (1974) 1
2. A. H. Walenta, J. Heintze and B. Shurlein, Nucl. Instr. and Meth. 92 (1972) 373
3. C.J. Barkowski and M.K. Kopp, IEEE Transactions, Nucl. Sci. NS-17, 340 (1970)
4. D.M. Lee, S.E. Sobottka, H.A. Thiessen, Nucl. Instr. and Meth. 120 (1974) 153-156
5. V. Perez-Mendez and S. Parker, IEEE Transactions, Nucl. Sci. NS-21, No. 1 (1974) 45
6. J. Alberi, J. Fisher, V. Radeka, L.C. Rogers and B. Schoenborn, IEEE Transactions, Nucl. Sci. Vol. NS-22 (1975) 255
7. A. Breskin, G. Charpak, B. Gabiod, F. Sauli, N. Trautner, W. Duinker and G. Schultz, Nucl. Instr. and Meth. 119 (1974) 9-28
8. M. Atac and C. Ankenbrandt, IEEE Transactions Nucl. Sci. NS-22, No. 1 (1975) 306
9. T.S. Nigmanov, V.P. Pugachevich, V.D. Riabtsov, M.D. Shafranov, E.N. Tsyganov, D.V. Uralsky, A.S. Vodopianov, F. Sauli, M. Atac and J. Tompkins, Fermilab Internal Report, 76/26-EXP (1976)
10. M. Atac, R. Bosshard and Y. Kang, Fermilab Internal Report, FN-286 (December 1975)
11. R. Bosshard, R.L. Chase, J. Fisher and V. Radeka, BNL Internal Report No. 19982, Proceedings of 2nd ISPRA Nucl. Elec. Symp. (1975) EURATON 5370e, 145-149
12. G. Amsel and R. Bosshard, Rev. of Sci. Instr., Vol. 41, No. 4 (1970), 503-514; R.L. Wigington and N.S. Nahman, PIRE 45 (1957) 166

FIGURE CAPTIONS

- Figure 1 The cross-sectional view of the chamber.
- Figure 2 (a) A descriptive view of the delay line strip.
- Figure 2 (b) Schematic diagram of the current loops.
- Figure 3 A spectrum of 5.9keV x-ray line of Fe⁵⁵ and 2.8keV Argon escape line.
- Figure 4 The circuit diagram of the current amplifier.
- Figure 5 (a) Pulses obtained from the sense wire. Horizontal scale is 20 nsec/cm and vertical scale is 50mV/cm.
- Figure 5 (b) Pulses obtained from the delay line. Horizontal scale is 20nsec/cm and vertical scale is 10mV/cm.
- Figure 6 Delay time spectra from the difference time measurements.
- Figure 7 Time delay as a function of mean source positio
- Figure 8 Overall view of the set-up at the beam line.
- Figure 9 Track position accuracy as a function of the track position along the delay line, determined from distributions (MWPC resolution not unfolded).
- Figure 10 Typical difference of delay line coordinate measurements and beam track MWPC measurements (wire spacing 1mm).

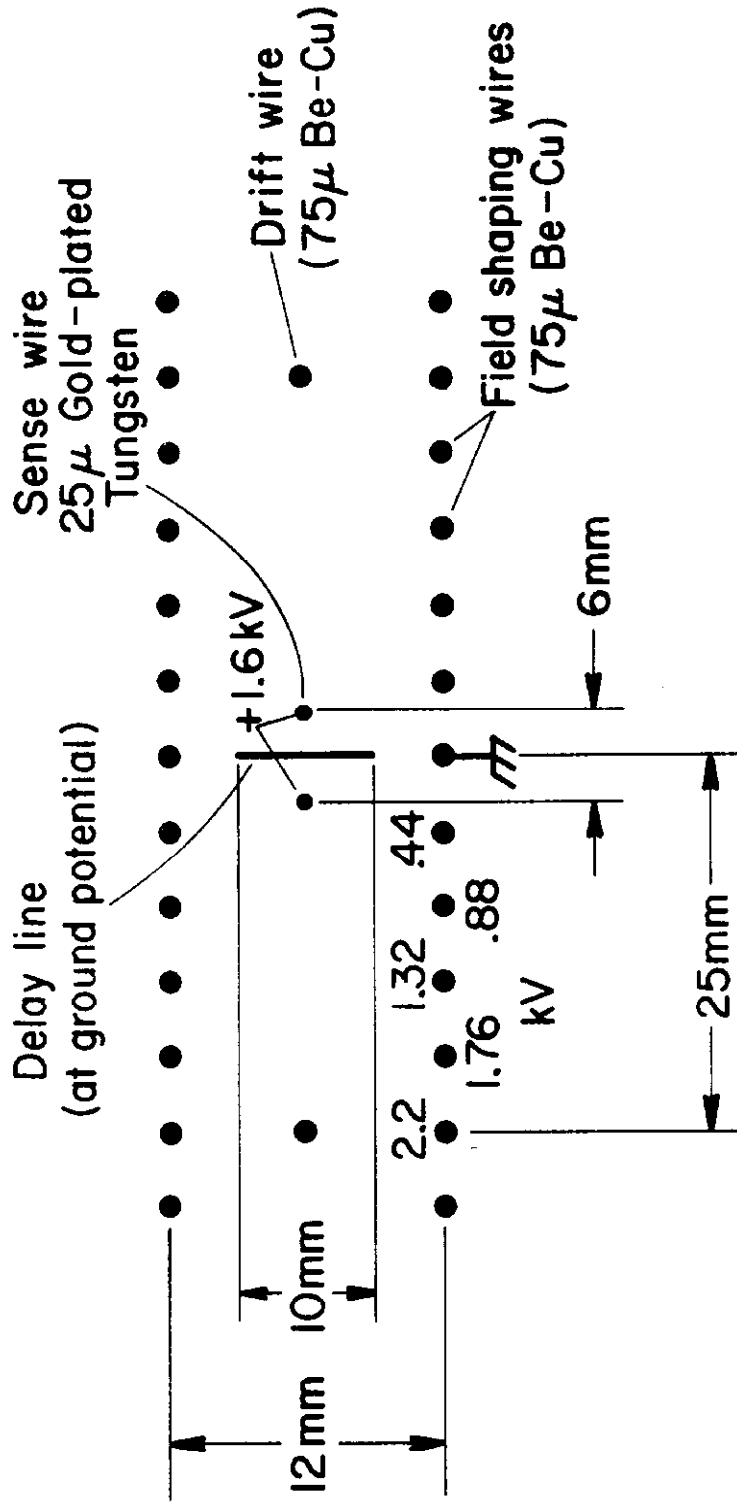
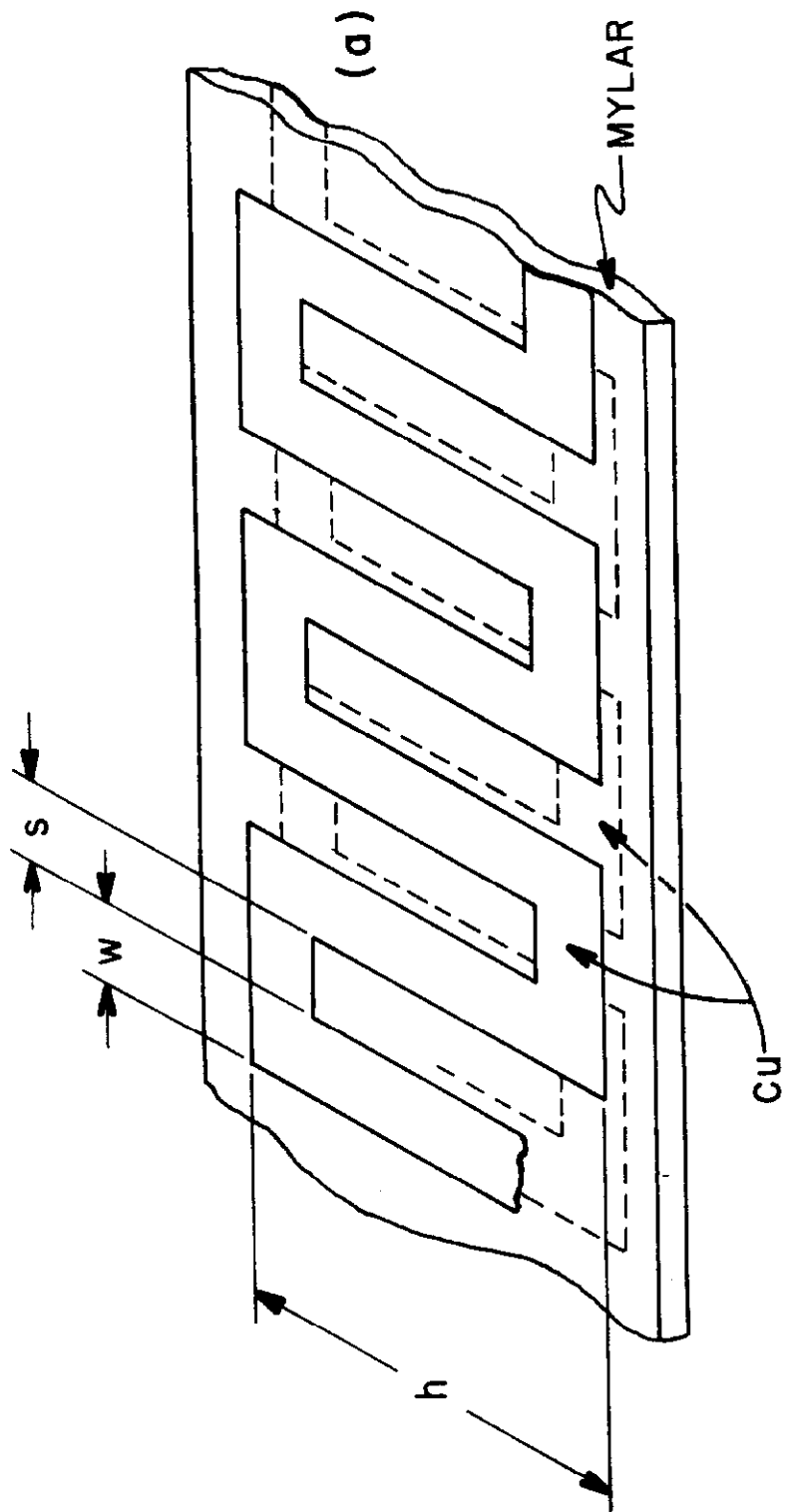


FIG. 1



$s = 275\mu$

$w = 250\mu$

$h = 9.5\text{mm}$

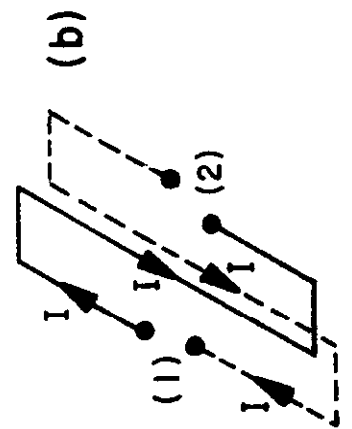


FIG 2

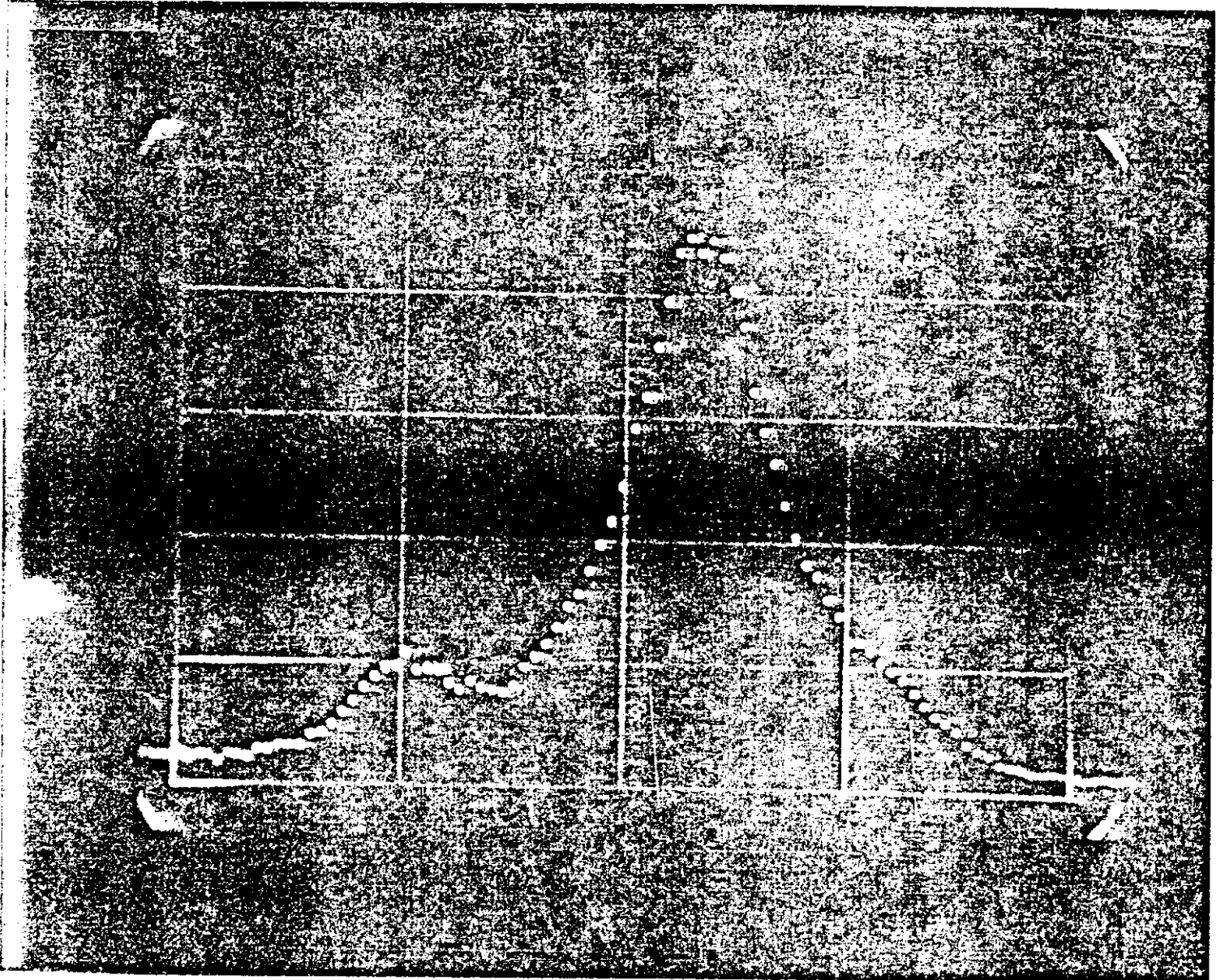
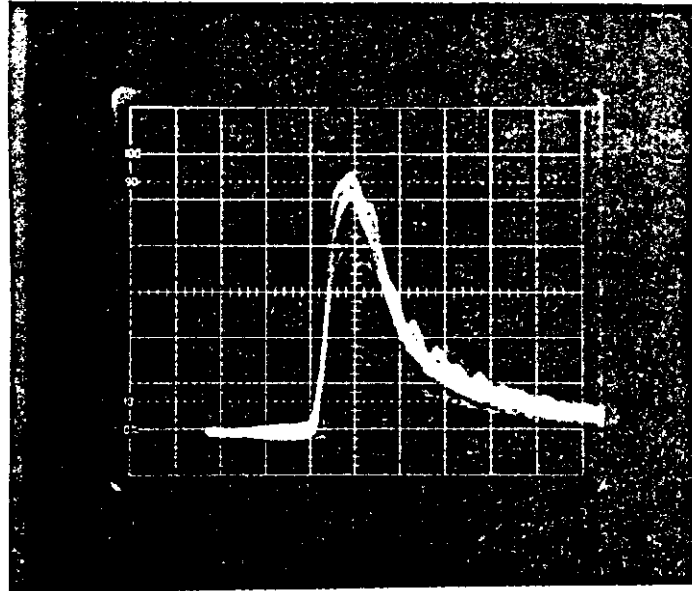
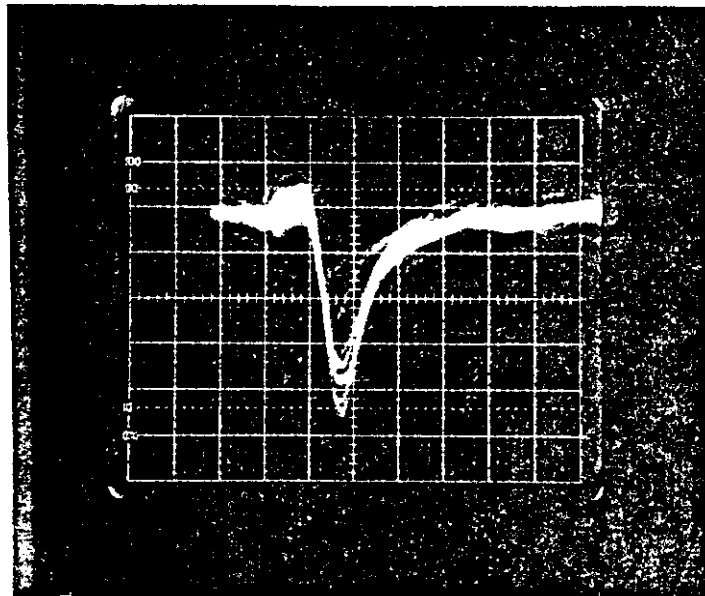


FIG. 3



a



b

FIG. 5

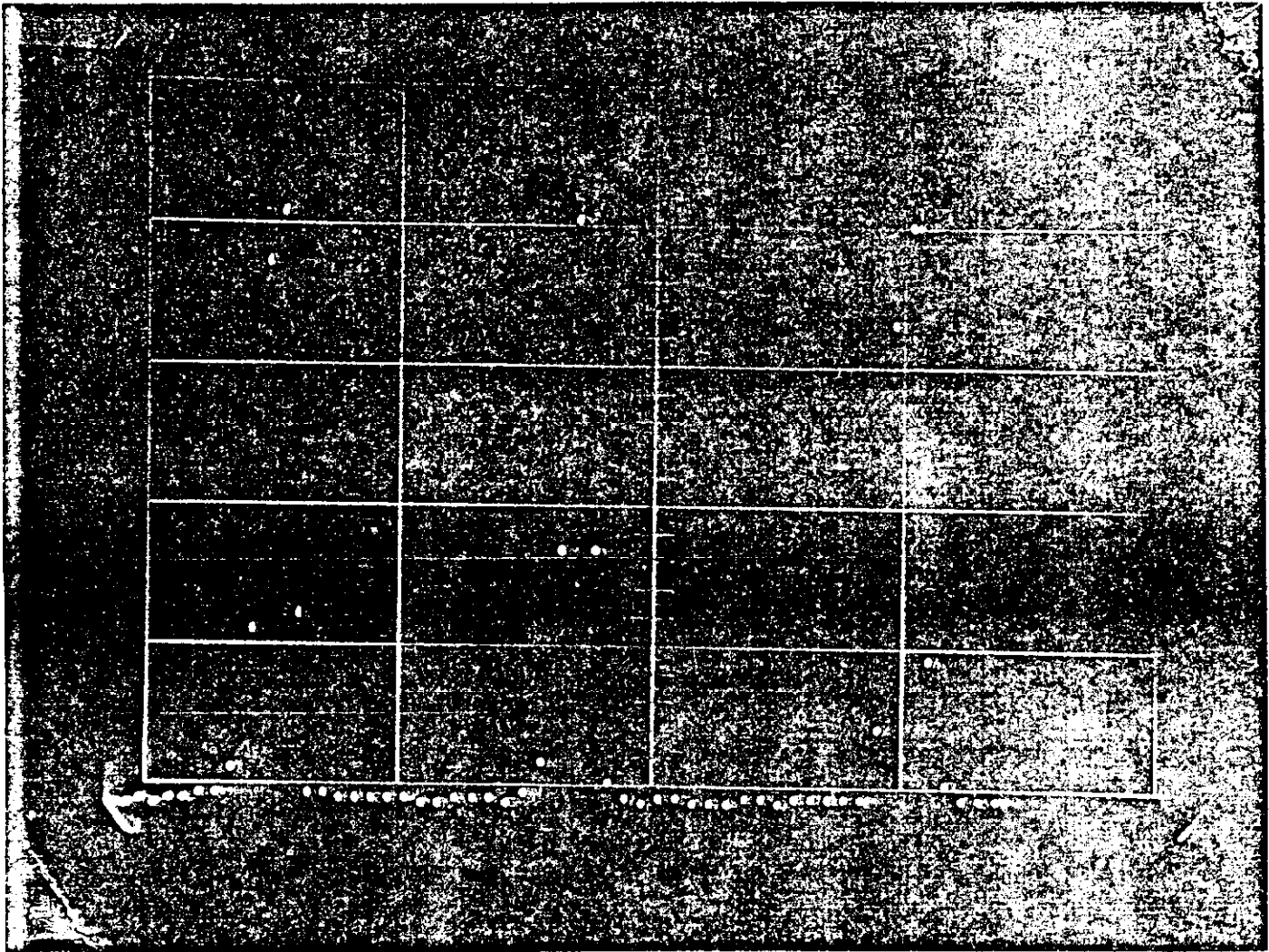


FIG. 6

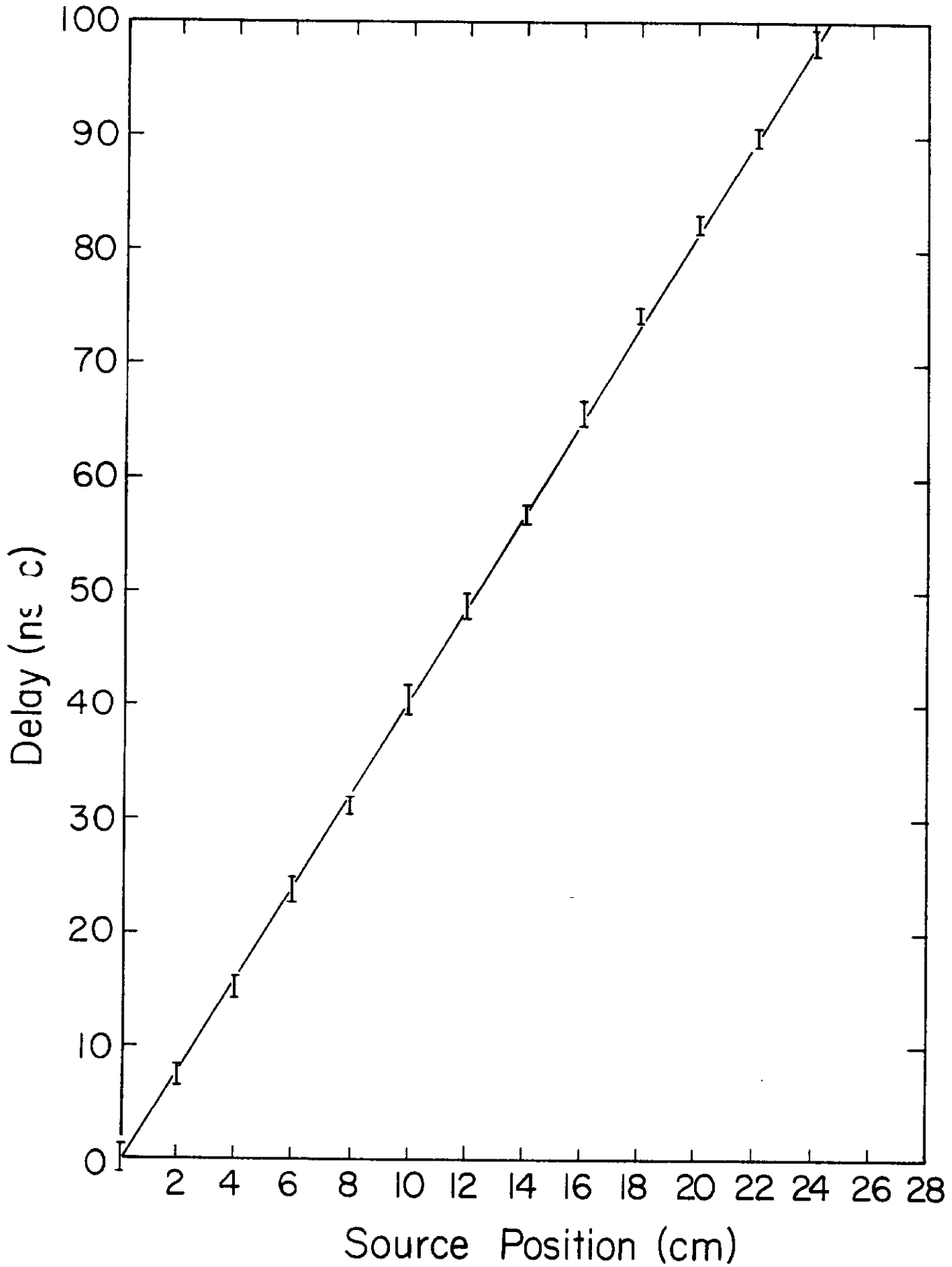


FIG 7

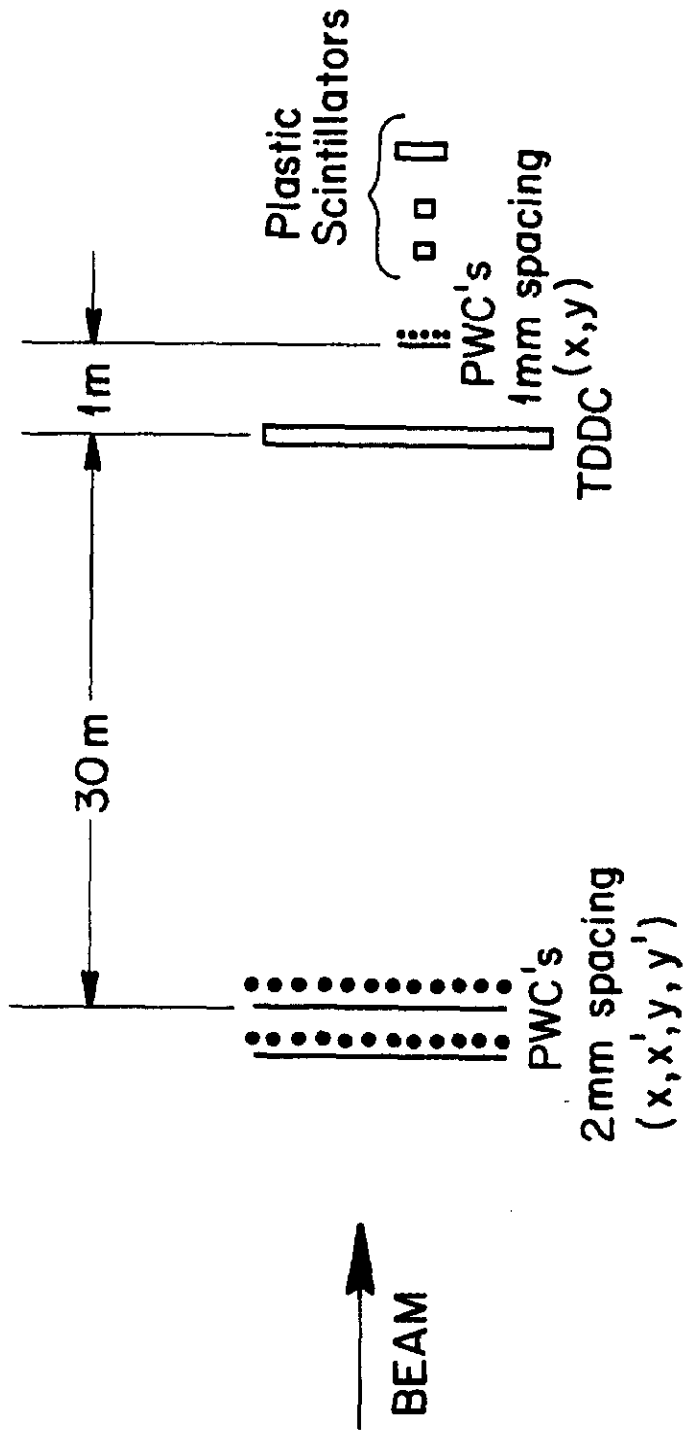
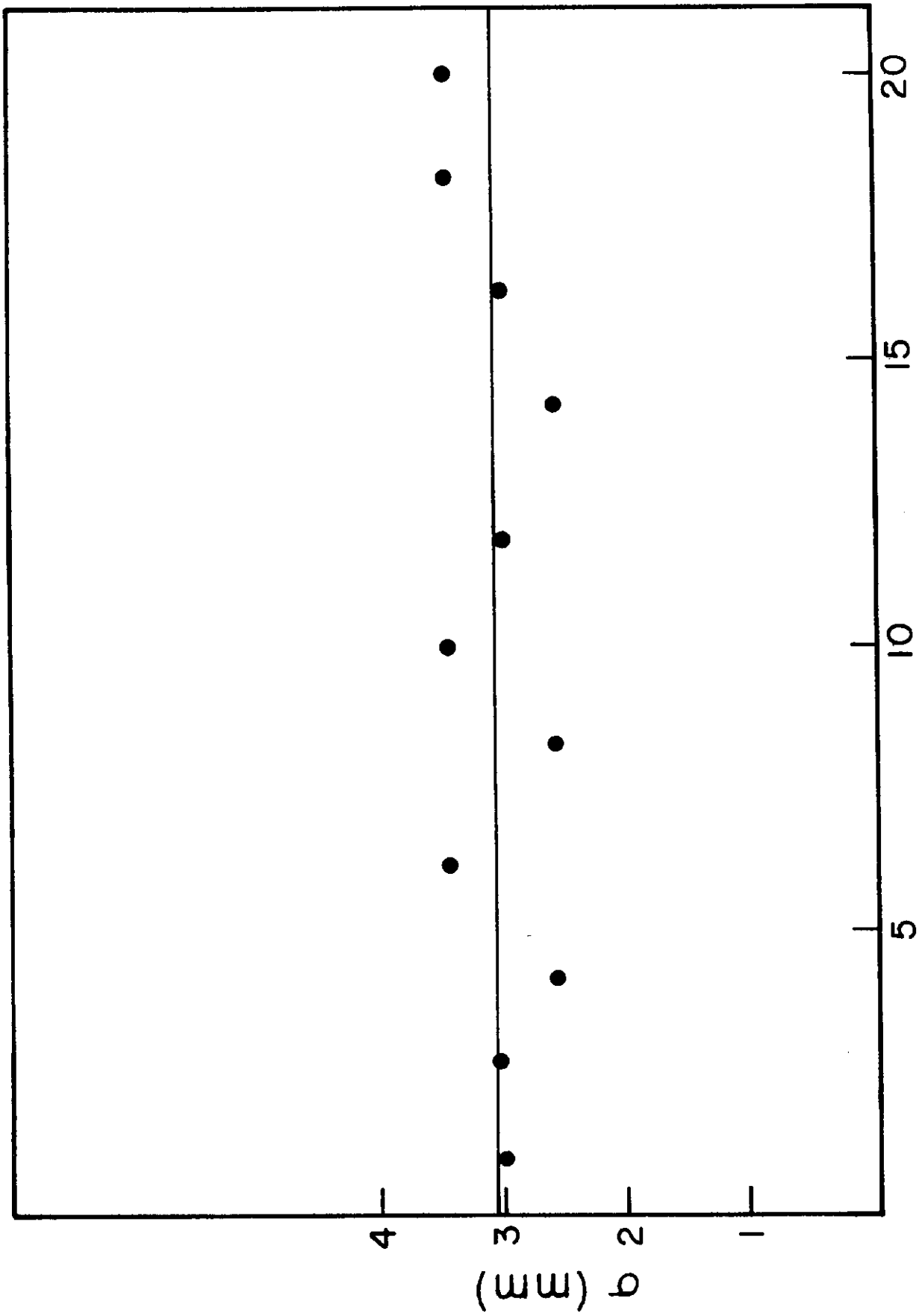


FIG. 8



Length Of Delay Line (cm)

FIG. 9

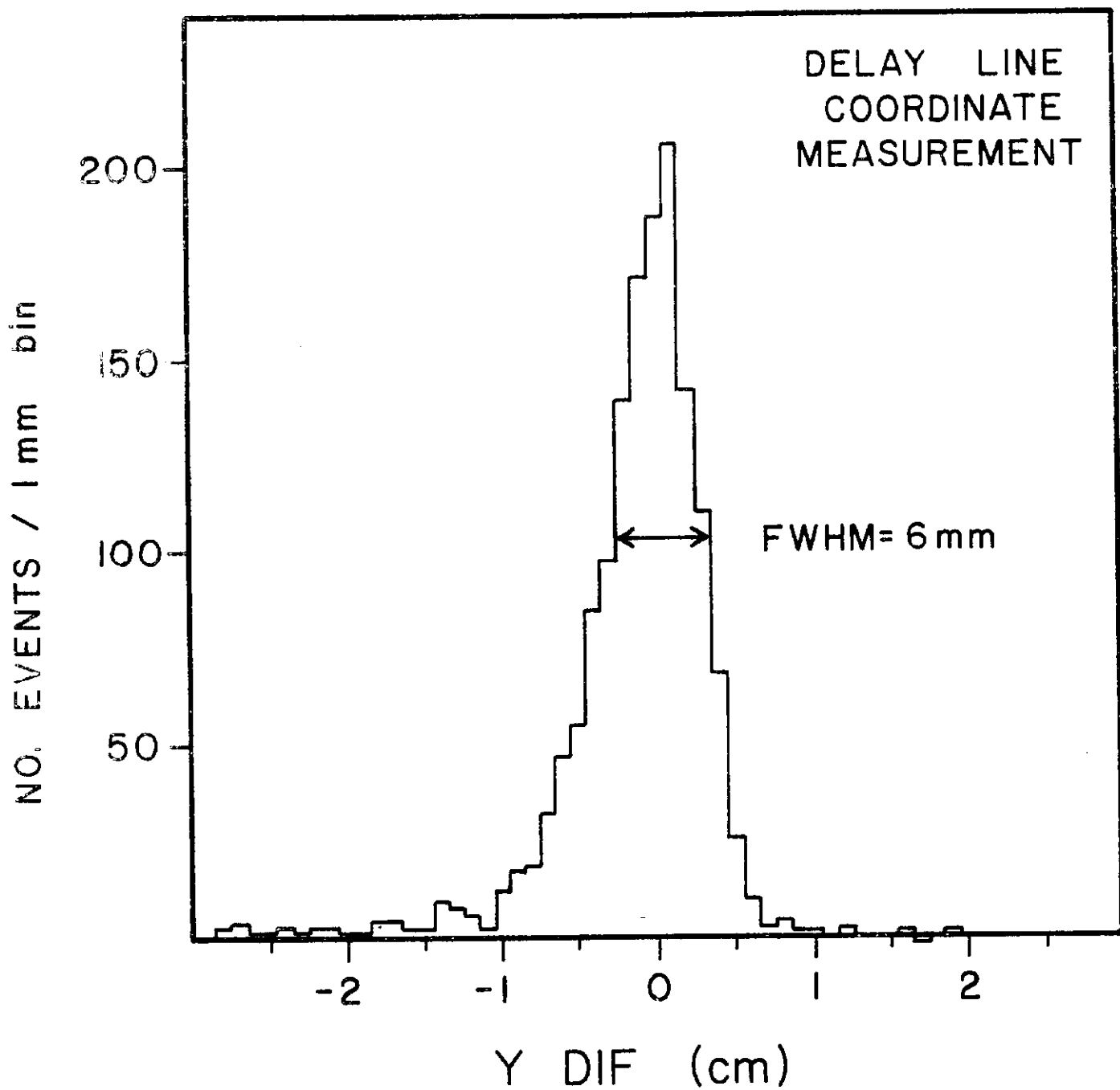


FIG. 10